Simple Modelling of Structured Optical Fibre Drawing

Ghazal Tafti[1]*, Wenyu Wang[1], Yanhua Luo[1], Kevin Cook[1, 2], John Canning[1, 2], Gang-Ding Peng[1]

[1]National Fibre Facility, Photonics & Optical Communication, School of Electrical Engineering and Telecommunications, University of New South Wales, Kensington, NSW 2052, Australia

[2]interdisciplinary Photonics Laboratories (iPL), School of Electrical & Data Engineering, UTS and School of Chemistry, The University of Sydney, NSW 2007 & 2006 Australia

Author e-mail address: g.fallahtafti@student.unsw.edu.au, wenyu.wang@student.unsw.edu.au, yanhua.luo1@unsw.edu.au, Kevin.Cook@uts.edu.au, John.Canning@uts.edu.au, g.peng@unsw.edu.au

Abstract: The role of internal capillary structure on optical fibre drawing is explored. A modified single-capillary function to cater for multi-capillary structural constraint within a larger single capillary draw is proposed and shown to give reasonable fits with experiment.

OCIS codes: (060.4005) Microstructured optical fibres; 060.5295 Photonic crystal fibers;

1. Introduction

The structure of structured optical fibres (SOF) [1(a)-(d)] is usually characterised by periodic arrays of microscopic air-holes running along its entire length. Changes in the size and distribution of the air-holes can significantly alter the optical properties of SOFs. This provides flexibility in design and allows for the development of SOFs with important features, including endlessly single-mode [1(b)], high-nonlinearity [1(d)] and temperature-independent high-birefringence [2]. The design and fabrication of SOFs are of interest in telecommunications [3], optical fibre sensing [4(a), (b)], and fibre lasers [5(a), (b)]. The final structure of SOF depends on the drawing process which involves a complex interplay between furnace temperature, pressurisation, drawing tension, feeding rate and drawing speed. Changes in these parameters or conditions directly affect the viscosity flow, surface tension, and shear force. They can significantly alter the air hole geometry and hence the properties of the fibre.

Although numerous papers describe the fabrication process of SOFs, there have been only a few research studies attempted to rigorously investigate the effects of drawing parameters [6(a)-(d)]. Several models based on the Navier-Stokes and convection-diffusion equations have been developed to describe the fluid flow in the neck-down region at the drawing process [7(a)-(c)]. Fitt *et al*. [7(b)] used a simplified model to describe the drawing process of a hollow fibre with a single axisymmetric hole, relating it to an idealized single capillary. They compared their solution with the experimental results of drawing a single capillary to verify their model at different drawing pressures. Later, a number of studies have been conducted using this single capillary analogy to purportedly predict the fabrication process of SOFs. A fundamental problem with this approach is that the arbitrary fitting of a single capillary model to experimental data has no clear physical justification because there is no reason why the internal multi-capillary structure of the SOF can be ignored.

This paper aims to modify the simple capillary model to make it suitable for analytical SOF studies by taking into account the internal structure. The SOF studied is composed of four hexagonal rings of air-holes surrounding the solid-core. A comparison between the experimental and predicted results is presented. The effect of a net counter-pressure from the surrounding holes on an air-hole within the drawn SOF is the likely explanation for the difference. A simple intuitive modification of the Fitt's single capillary approach, using a structural constraint to capture the role of the multiple-capillary structure within the SOF, is shown to be sufficient opening a pathway to quantify constraint and optimise actual SOF design.

2. Design and Fabrication of Structured Optical Fibres

There are several methods to fabricate SOFs including stacking of capillaries [6 (a)-(d)], extrusion, [8(a)], sol-gel casting [8(b)], drilling [8(c)-(e)] and potentially the most disruptive and flexible of all, 3D printing [9(a), (b)]. The capillary stacking technique, the most widely adopted method, is used in this study. Stacking allows relatively fast, low-cost, clean, and flexible fabrication although it has significant limitations on design flexibility beyond periodic arrays. The SOF we draw for this work is made up ot capillaries (inner diameter ϕ_c = 1.56 mm) stacked to form a hexagonal pattern, inserted into the jacketing tube. The interstitial spaces situated between the capillaries were removed by fusing on a modified chemical vapor deposition (MCVD) lathe. The fused preform was drawn into SOFs using an optical fibre drawing tower (furnace heating zone length L = 4 cm). Feeding rate, drawing speed, furnace temperature, and drawing pressure were adjusted to control the shape and structure of SOFs. Drawing pressure controlled air-holes' dimensions by adjusting collapse or expansion.

3. Single Capillary Draw Analogy

Fitt *et al*. [7(b)] used a simplified closed-form Navier Stokes expression and convection-diffusion equations that govern the viscous fluid flow in the neck down region of a furnace drawing capillary (Figure 1(a)).

The model takes into account the interplay between furnace temperature, pressurisation, drawing tension, feeding rate, and drawing speed. According to this single capillary model, the inner radius of the drawn capillary h (m) is defined as a function of drawing parameters by [7(b)]:

$$h(x) = \exp\left(\frac{-\beta x}{2L} - P\,exp\left(\frac{-\beta x}{L}\right)\right)\left[h_{10}\exp(P) - \int_0^x G\exp\left(\frac{-\beta u}{2L} + Pexp\left(\frac{-\beta u}{L}\right)\right)du\right] \quad (1)$$

where $G = \gamma/(2\mu v_f)$, $\beta = log(v_d/v_f)$, $P = LP_d/(2\beta\mu v_f)$, viscosity μ (N·s·m^{-2}), surface tension is γ (N·m^{-1}) and preform feeding speed is v_f (m·s^{-1}). The drawing speed is v_d (m·s^{-1}), and the drawing pressure applied to the air-holes within the preform is P_d (N·m^{-2}). L (m) is the furnace heating zone length whilst h_{10} (m) is the inner radius of the capillary and x (m) is the distance along the axis of a capillary from the start point of the neck-down region. The surface tension of the silica γ = 0.3 N/m. The viscosity of the silica, is given approximately by $\mu = 0.1 \times 10^{-6.24+26900/(T+273)}$ where T is the drawing temperature (°C) [10]. In this model, the length of the heating zone is assumed to be much larger than the radius of the outer capillary, h_{20}, so $h_{20}/L \ll 1$. Theoretically, there exist two pressure thresholds, collapse $P_{d,coll}$ and expansion $P_{d,exp}$, that determine capillary collapse ($P_d < P_{d,coll}$) and expansion ($P_d > P_{d,exp}$), respectively, satisfying [7(b)]:

$$G\int_0^x \exp\left(\frac{-\beta u}{2L} + \frac{LP_{d,coll}}{2\beta\mu v_f} exp\left(\frac{-\beta u}{L}\right)\right) du = h_{10} \exp\left(\frac{LP_{d,coll}}{2\beta\mu v_f}\right) \quad (2)$$

$$P_{d,exp} > \frac{\gamma}{h_{10}} + \frac{\beta\mu v_f}{L} \quad (3)$$

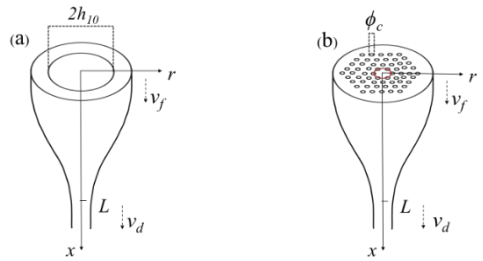

Figure 1 Illustration of (a) a single capillary with $\phi_{inner} = 2h_{10}$;(b) hexagonal SOF with $\phi_{inner} = \phi_c$ at the neck-down region.

An obvious difference between the SOF and the single capillary model is the role of the multi-capillary internal structure inside the main outer capillary structure of the fibre – this difference exists because each capillary expands in its own right against each other creating a cylindrical web with an effective counteracting pressure that should lead to an overall pressure differing from that of the single capillary analogy. Here, we quantify the difference between the single capillary and the actual SOF without making assumptions on parameters to obtain an arbitrary fit. More importantly, this difference should be a direct measure of the degree of constraint in the structure since it is what causes the deviation from a singular capillary of similar dimensions.

4. Experimental and Predicted Results and Discussion

To study the relation between the drawing conditions and the final air-hole dimensions/structures of SOFs, drawing temperature, T_d, drawing pressure, P_d, preform feeding speed, v_f, and drawing speed, v_d, were adjusted. Velocities v_f and v_d were set at v_f = 0.5 mm/min and v_d = 15 m/min to produce a hexagonal pattern of air-holes in the fibre cross-section with outer diameter $\phi_f \approx$ 125 µm. The air-hole size in a SOF can be tuned by adjusting P_d and/or T_d. P_d can also be changed indirectly through v_d which changes drawing tension and therefore internal pressure via Poisson's ratio. The response of control by T_d is slow but that by P_d is fast. Therefore, P_d is explored as a suitable parameter for controlling the eventual air-hole structure of SOFs. To maintain a desirable level of surface tension, whilst not making the fibre brittle at too low T_d, the furnace temperature had to lie between 1855 < T < 1880 °C. Here, T_d = (1860 – 1870) °C and P_d = (0.1 - 16) mbar were considered.

Scanning electron microscopy (SEM) and optical microscopy were used to image the SOFs. Image analysis characterised the fibre geometry and determined the air-hole size. The average size of the air-holes in the first ring from the core is used for comparison (Figure 1(b)). One would expect the changes in dimension here to be approximated by a constrained single capillary with a diameter close to that of the ring diameter. Figure 2(a) shows the experimental results from the SOF drawn and also the results for a single capillary analysis (FM) under different drawing pressures at T_d = 1860 °C. The collapse and expansion pressure thresholds of a single drawn capillary were calculated from Eqs (2) and (3). Within experimental error there is good agreement between experimental and predicted results prior to rapid expansion (i.e. when the effective ring of holes starts to expand rapidly). However, when $P_d > P_{d,exp}$, the size of the air-hole predicted by the Fitt model deviates significantly from that of the experimental results.

(a)

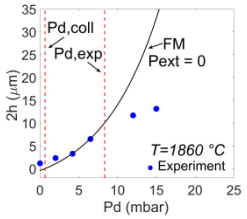

(b)

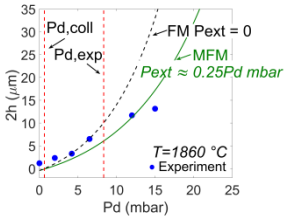

Figure 2. Experimental vs predicted results of the Fitt model at T_d = 1860 °C, P_d = (0.1-16) mbar: (a) Ignoring P_{ext} and (b) with $P_{ext} \approx 0.25P_d$.

To model the system in its entirety using a multi-capillary model would be extremely complicated. Considering that the net effect of the structure is to oppose the expansion from the beginning, we can introduce an external pressure P_{ext} to quantify the net counter-pressure to a hole's expansion from the lattice holes in the SOF structure. The value of P_{ext} depends on the position of the air-holes in the SOF, the size of the holes, and the internal drawing pressure. Hence in a multiple air-hole SOF, the effective draw pressure, $P_{d,eff}$ ($P_{d,eff} = P_d - P_{ext}$) determines a hole's size, corresponding to P_d in a single capillary structure. By apply this $P_{d,eff}$ we introduce the modified single capillary model (MFM) for SOF, providing a simple, intuitive and direct measure of multiple capillary structure contributions, which define a so-called structural constraint parameter, SC, that can be used to optimise designs. In terms of the normalized pressure parameter P_{SC} :

$$P_{SC} = L(P_d - P_{ext})/(2\beta\mu v_f) \tag{4}$$

Based on this modified single capillary model, the external pressure P_{ext} will increase the expansion limit by:

$$P_{d,exp} > \frac{\gamma}{h_{10}} + \frac{\beta\mu v_f}{L} + P_{ext} \tag{5}$$

in which $P_{d,exp}$ is the internal drawing pressure leading to expansion of the entire structure. From the experimental results, this external pressure can be defined as a function of the internal drawing pressure and predicted to be $P_{ext} \approx 0.25P_d$, as shown in Figure 2(b).

Furthermore, Figure 3 (a) and (b) show the experimental results and the predicted results at different drawing conditions T_d = 1865 °C and 1870 °C, v_f = 0.5 mm/min, v_d = 16.5 m/min, respectively. Seen from Figure 3, good agreement is also observed between the experimental and predicted results by using $P_{ext} \approx 0.25P_d$.

(a)

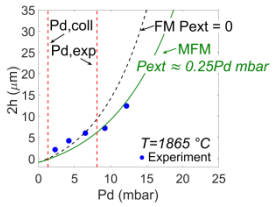

(b)

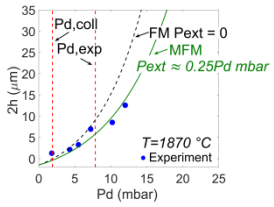

Figure 3. Experimental vs predicted results of the single capillary model at P_d = (0.1-16) mbar: (a) T_d = 1865 °C and (b) T_d = 1870 °C.

5. Conclusion

Using a modified single-capillary function, we propose a simple analytical approach to model SOF structure with regard to drawing parameters and conditions. A single capillary analogy alone is insufficient because it ignores the expected contribution from an effective counter pressure arising from the multi-capillary interior. However, in order to retain the simplicity of the single capillary approach whilst being able to describe the actual pressures for a multi-capillary system of the type in a SOF, the single capillary model has been modified to include a structural constraint parameter arising from the internal capillary structure. This assumes the dominant force on the fibre remains the net expansion of the entire system with the structure acting as a constraint, consistent with observations. An effective external pressure was defined and added to the single capillary model leading to good agreement between the experimental and predicted results for the situation explored here, when external pressure is close to ¼ of drawing pressure. The model retains simplicity but has physical meaning supporting it with structural constraint as a direct measure of interest for the study of SOFs. It can therefore be used to explore and quantify the variations in SC arising with different patterns, and obtain information that will relate to the ability to tune, for example, stresses and strains in the final fibre. In our experiments, SOFs were fabricated under different drawing conditions and the structure-related results are shown to give agreement with the simple analytical fit. Further refinements are possible by closely studying the regime below rapid expansion in more detail and exploring the impact of different hole sizes and designs.

Acknowledgment: The authors thank the Asian Office of Aerospace R&D for the grant (FA2386-16-1-4031).

6. References

1. (a) J. Knight *et al.*, Opt. Lett. **21**, 1547 (1996); (b) T. Birks *et al.,* Opt. Lett. **22**, 961 (1997); (c) R. Buczynski, Acta Phys. Pol. A **106**, 141 (2004); (d) J. Stone, Ph.D. dissertation (Physics, University of Bath, 2009).
2. A. Michie *et al.*, Opt. Express **12**, 5160 (2004).
3. T. Matsui *et al.*, J. Lightwave Technol. **27**, 5410 (2009).
4. (a) A. Michie *et al.*, Meas. Sci. Technol. **18**, 3070 (2007); (b) T. Chen *et al.*, Opt. Lett. **36**, 3542 (2011).
5. (a) K. Cook *et al.*, J. Electron. Sci and Technol of China **6**, 442 (2008); (b) N. Groothoff *et al.*, Opt. Express **13**, 2924 (2005).
6. (a) G. Tafti *et al.*, 3rd Aust. & NZ Conf. Optics & Photon.(ANZCOP) (Queenstown, NZ 2017), Paper 142; (b) K. Lyytikainen *et al.*, Opt. Internet & Aust. Conf Opt. Fibre Tech., (Melbourne, 2003), 137; (c) K. Lyytikäinen, Ph.D. dissertation (Physics, OFTC, Univ. Sydney, 2004); (d) W. Wang *et al.*, 3rd Aust. & New Zealand Conf. Opt. & Photon,, (ANZCOP, NZ: Queenstown, 2017), Paper 141
7. (a) K. Lyytikainen *et al.*, in Microwave and Optoelectronics Conf., (Brazil, Iguaza Falls, 2003), pp. 1001; (b) A. Fitt *et al.*, J. Eng. Math. **43**, 201 (2002); (c) Y. Chen & T. Birks, Opt. Mater. Express **3**, 346 (2013).
8. (a) H. Ebendorff-Heidepriem & T. Monro, "Opt. Express **15**, 15086 (2007); (b) Y. Zhu *et al.*, Opt. Com. **281**, 55 (2008); (c) R. Kostecki *et al.*, Opt. Materials Express **4**, 29 (2014); (d) A. Denisov *et al.* Quantum Electron. **46**, 1031 (2016); (e) J. Canning *et al.*, Opt. Express **11**, 347 (2003)
9. (a) K. Cook *et al.,* Opt. Lett. **40**, 3966 (2015); (b) J. Canning *et al.*, Asia Comm. Photon Conf., (Hong Kong, 2015), Paper ASu4B.2
10. N.P. Bansal & R.H. Doremus, in *Handbook of Glass Properties*, (Academic Press, New York 1986).